ACS OMEGA

http://pubs.acs.org/journal/acsodf Article

Asymmetric Assembly of Chiral Lanthanide(III) Tetranuclear Cluster Complexes Using Achiral Mixed Ligands: Single-molecule Magnet Behavior and Magnetic Entropy Change

Cai-Ming Liu* and Xiang Hao

Cite This: *ACS Omega* 2022, 7, 20229–20236 Read Online

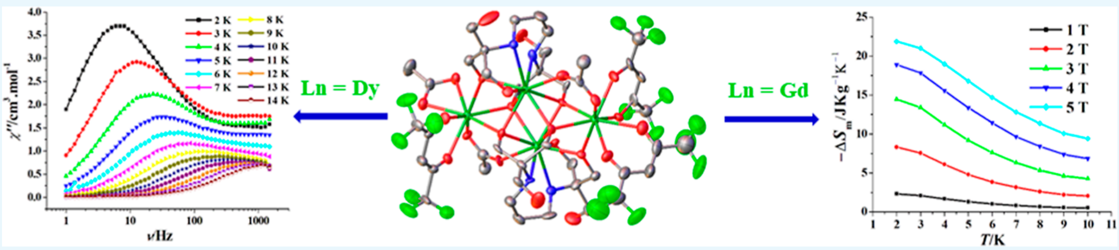

ABSTRACT: It is challenging to use achiral ligands to spontaneously construct chiral molecular magnets. In this work, two new Ln_4 cluster complexes based on *N*,*N*′-(1,3-propanediyl)bis[*N*-[1,1-bis(hydroxymethyl)-2-hydroxyethyl]amine] (H_6L) have been assembled, which are crystallized in a chiral space group due to the asymmetric distribution of acetate (OAc^-) groups and hexafluoroacetylacetonate (F_6acac^-) groups on both sides of the parallelogram-like Ln_4 core. Complex **1**, $[Dy_4(H_3L)_2(OAc)_3(F_6acac)_3]\cdot 5MeOH\cdot 2H_2O$, exhibits single-molecule magnet properties at the zero field with the U_{eff}/k value of 48.4 K; notably, besides the Orbach process, the Raman process is also prominent for the magnetic relaxation of **1**. Complex **2**, $[Gd_4(H_3L)_2(OAc)_3(F_6acac)_3]\cdot 4MeOH\cdot 2.5H_2O$, displays a large magnetocaloric effect, whose largest $-\Delta S_m$ value is 21.88 J kg^{-1} K^{-1} (when T = 2 K and ΔH = 5 T); it thus can be utilized as a good magnetic refrigeration molecular material.

■ INTRODUCTION

Recently, lanthanide(III) cluster complexes have attracted great attention in the field of single-molecule magnets (SMMs)[1] and magnetic refrigeration molecular materials,[2,3] which is closely related to the large spin value of lanthanide(III) ions. If the specified lanthanide(III) ions such as dysprosium(III) ions have strong magnetic anisotropy, they are suitable for the construction of SMMs, and when the specified lanthanide(III) ions are gadolinium(III) ions, they are suitable for the assembly of magnetic refrigeration molecule materials, owing to the largest ground state spin value (S_{Gd} = 7/2) and no magnetic anisotropy.[4,5] Because the magnetic axis and the symmetry of each dysprosium(III) ion in the cluster complex are difficult to control,[6] the research progress of dysprosium(III) cluster complexes in the SMM field is relatively slow. However, gadolinium(III) cluster complexes have obvious advantages in the study of magnetic refrigeration molecular materials.[7−12]

On the other hand, if chirality is introduced into molecular magnets, it will bring valuable physical properties such as nonlinear optics,[13−16] ferroelectricity,[17−20] and magneto-optical effects,[21−27] making them attractive multifunctional molecular materials. The general case is to obtain chiral structured molecule-based magnets by chiral ligand coordination[28−37] or even by cocrystallizing with chiral organic molecules.[38] Another more challenging case is to use achiral ligands to spontaneously construct chiral structured molecule-based magnets, which involve helical chirality,[39] Δ/Λ octahedral coordination configuration of transition metal ions,[40] and cooperative orientation of anions and cations in the axial direction.[41] It is well known that the chirality occurs when different functional groups are attached to the carbon atom in organic chemistry, however, the chirality of cluster SMMs through the asymmetric distribution of different achiral ligands on both sides of the cluster core has never been reported.

Lanthanide(III) tetranuclear clusters with various core structures, which include chain, square, butterfly or rhombus, and cube, might be the most studied clusters in SMMs.[42−56] They can not only exhibit large energy barrier values but also can be used to study multistep magnetic relaxation behavior. Recently, we constructed a parallelogram-like Dy(III) tetrametallic SMM, $[Dy_4(H_3L)_2(OAc)_6]\cdot 2EtOH$,[57] using

Received: April 6, 2022
Accepted: May 11, 2022
Published: June 3, 2022

acetate ligands and the bis-tris propane ligand, that is *N*,*N*′-(1,3-propanediyl)bis[*N*-[1,1-bis(hydroxymethyl)-2-hydroxyethyl]amine] (H_6L, Scheme 1). Interestingly, we further found that if another ligand, hexafluoroacetylacetonate anion (F_6acac^-), was added, we could obtain Ln(III) tetranuclear clusters (Ln = Dy and Gd) crystallized in a chiral space group. Herein we report the room-temperature syntheses, X-ray crystal structures, SMM properties, and magnetic entropy changes of two chiral Ln(III) tetranuclear clusters with the *N*,*N*′-(1,3-propanediyl)bis[*N*-[1,1-bis-(hydroxymethyl)-2-hydroxyethyl]amine] ligand, the acetate ligand, and the hexafluoroacetylacetonate ligand. $[Dy_4(H_3L)_2(OAc)_3(F_6acac)_3]\cdot 5MeOH\cdot 2H_2O$ (**1**) and $[Gd_4(H_3L)_2(OAc)_3(F_6acac)_3]\cdot 4MeOH\cdot 2.5H_2O$ (**2**), both have a parallelogram-like Ln_4 cluster core: complex **1** shows SMM properties at the zero field, while complex **2** displays a large magnetocaloric effect.

Scheme 1. Molecule Structure of the Bis-tris Propane Ligand (H_6L)

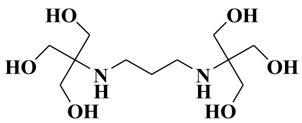

■ EXPERIMENTAL PROCEDURES

$Dy(F_6acac)_2Ac\cdot 2H_2O$ and $Gd(F_6acac)_2Ac\cdot 2H_2O$ were presynthesized by the method described in the literature.[58−60]

Preparation of 1. H_6L (0.125 mol), $Dy(F_6acac)_2Ac\cdot 2H_2O$ (0.25 mmol), $LiOH\cdot H_2O$ (0.50 mmol), and 20 mL of methanol were added to a 50 mL Erlenmeyer flask and stirred for 5 h to obtain a colorless solution. After filtration, the filtrate was left to slowly evaporate the solvent. Colorless small block single crystals of **1** were harvested in about ten days, which were washed with 10 mL of water and 10 mL of methanol in turn, and were then air-dried naturally. Yield (calculated based on Dy): 35%. Anal. calcd for $C_{48}H_{80}Dy_4F_{18}N_4O_{31}$ (**1**): C, 26.19; H, 3.66; N, 2.55%. Found: C, 26.23; H, 3.69; N, 2.52%. IR (KBr, cm^{-1}): 3674 (w), 3397 (br s), 2936 (w), 2884 (w), 1661 (s), 1559 (s), 1529 (m), 1502 (m), 1450 (m), 1347 (w), 1255 (s), 1206 (s), 1144 (s), 1100 (w), 1027 (m), 946 (w), 855 (w), 797 (w), 757 (w), 662 (m), 618 (w), 584 (w), 560 (w), 527 (w), 495 (w), 420 (w).

Preparation of 2. H_6L (0.125 mol), $Gd(F_6acac)_2Ac\cdot 2H_2O$ (0.25 mmol), $LiOH\cdot H_2O$ (0.50 mmol), and 40 mL of MeOH/CH_2Cl_2 (v/v = 1) were added to a 100 mL Erlenmeyer flask and stirred for 5 h to obtain a colorless solution. After filtration, the filtrate was left to slowly evaporate the solvent. Colourless small block single crystals of **2** were harvested in about ten days, which were washed with 10 mL of water and 10 mL of methanol in turn, and were then air-dried naturally. Yield (calculated based on Gd): 40%. Anal. calcd for $C_{47}H_{79}F_{18}Gd_4N_4O_{30.5}$ (**2**): C, 26.15; H, 3.69; N, 2.59%. Found: C, 26.11; H, 3.73; N, 2.54%. IR (KBr, cm^{-1}): 3676 (w), 3397 (br s), 2940 (w), 2887 (w), 1661 (s), 1559 (s), 1527 (m), 1502 (m), 1448 (m), 1348 (w), 1255 (s), 1206 (s), 1144 (s), 1096 (w), 1026 (m), 950 (w), 854 (w), 797 (w), 741 (w),728 (w), 662 (m), 618 (w), 584 (w), 557 (w), 527 (w), 489 (w), 412 (w).

■ RESULT AND DISCUSSION

Synthesis. The bis-tris propane ligand is a common polydentate ligand containing not only the N coordination site but also the O coordination site, which had been successfully used to assemble some 3d cluster complexes,[61,62] 3d-3d heteronuclear cluster complexes,[63,64] and 3d−4f heteronuclear cluster complexes.[65−67] We also recently used it to solvothermally react dysprosium acetate and lithium hydroxide in EtOH at 100 °C, yielding a dysprosium(III) tetranuclear cluster SMM, $[Dy_4(H_3L)_2(OAc)_6]\cdot 2EtOH$, which shows double magnetic relaxation behavior at the zero field.[57] In this study, we used the bis-tris propane ligand to react with $Ln(F_6acac)_2Ac\cdot 2H_2O$ (Ln = Dy and Gd) and lithium hydroxide in MeOH or (MeOH + CH_2Cl_2) for several hours at room temperature, and then slowly evaporated the solvent to obtain lanthanide(III) tetranuclear cluster compounds **1** and **2**. As expected, the hexafluoroacetylacetonate anion from the $Ln(F_6acac)_2Ac\cdot 2H_2O$ starting materials participates in the coordination acting as a terminal ligand, being assembled into the structures of complexes **1** and **2**, just like the acetate anion does. However, the molecules of complexes **1** and **2** contain three acetate groups and three hexafluoroacetylacetonate groups, and these different ligands have to be asymmetrically distributed on both sides of the Ln_4 cluster core, resulting in the loss of centrosymmetry of the entire molecule. Therefore, they are eventually crystallized in the chiral space group *P*1 (Table 1). Unfortunately, it is known from the process of single-crystal structure analysis that the two chiral isomers in **1** or **2** are combined in the form of twin crystals, so they cannot be separated manually under a polarizing microscope. In contrast, $[Dy_4(H_3L)_2(OAc)_6]\cdot 2EtOH$ is a centrosymmetric molecule crystallized in the centrosymmetric space group, *Pbca*,[57] because its six acetate anions are symmetrically

Table 1. Crystal Data and Structural Refinement Parameters for 1 and 2

	1	2
formula	$C_{48}H_{80}Dy_4F_{18}N_4O_{31}$	$C_{47}H_{79}F_{18}Gd_4N_4O_{30.5}$
F_w	2201.16	2159.14
crystal system	triclinic	triclinic
space group	*P*1	*P*1
a [Å]	11.0727(2)	11.1069(2)
b [Å]	12.9870(2)	12.9886(2)
c [Å]	13.6934(2)	13.7301(2)
α [deg]	69.304(2)	68.973(2)
β [deg]	89.4750(10)	89.2670(10)
γ [deg]	89.9360(10)	89.2490(10)
V [Å3]	1841.97(6)	1848.62(6)
Z	1	1
ρ_{calc} [g cm^{-3}]	1.984	1.939
μ [mm^{-1}]	4.138	3.667
T [K]	170	170
λ (Mo Kα) [Å]	0.71073	0.71073
reflections collected	46,806	47,985
unique reflections	14,449	13,077
observed reflections	13,257	11,850
parameters	955	954
GoF [$I \geq 2\sigma(I)$]	1.040	1.030
R_1 [$I \geq 2\sigma(I)$]	0.0262	0.0348
$_wR_2$ [$I \geq 2\sigma(I)$]	0.0601	0.0867
Flack parameter (twin)	0.413(19)	0.32(3)

https://doi.org/10.1021/acsomega.2c02155
ACS Omega 2022, 7, 20229−20236

distributed on both sides of the Dy_4 cluster core. This research suggests a new strategy to construct the chiral SMM by the asymmetric distribution of different achiral ligands on both sides of the cluster core.

Crystal Structures. The structures of cluster compounds **1** and **2** are very similar (Figure 1), and we, thus, focus on describing the crystal structure of **1**. As shown in Figure 1a, complex **1** has an approximately parallelogram-shaped Dy_4 core, with the Dy···Dy side lengths of 3.534, 3.822, 3.532, and 3.818 Å, respectively. Two bis-tris propane ligands each provide two η^3-CH_2O^- oxygen atoms to bridge the four planar Dy^{3+} ions from above and below, using the $\eta^3:\eta^3:\eta^1:\eta^1:\eta^1:\eta^2:\mu_4$ coordination mode observed in the SMM $[Dy_4(H_3L)_2(OAc)_6]\cdot 2EtOH$.[57] Such a $[Dy_4(OCH_2-)_4]$ core is very similar to that in $[Dy_4(H_3L)_2(OAc)_6]\cdot 2EtOH$.[57] The Dy2 atom and the Dy3 atom are both nine-coordinated, which are coordinated by one bis-tris propane ligand providing four oxygen atoms and two nitrogen atoms, another bis-tris propane ligand offering two η^3-CH_2O^- oxygen atoms, and one η^2-AcO^- ligand supplying one oxygen atom. By SHAPE software[68] analysis, it can be seen that the coordination configurations of these two Dy(III) ions are both spherical capped square antiprisms, and the deviation values from the C_{4v} symmetry are 1.029 for the Dy2 atom (Table S1) and 0.952 for the Dy3 atom (Table S2). However, both the Dy1 and Dy4 atoms are eight-coordinated: the Dy1 atom is bonded by one oxygen atom of the η^3-CH_2O^- group and one oxygen atom of the η^2-CH_2O^- group from one H_3L^{3-} ligand, one oxygen atom of the η^3-CH_2O^- group from another H_3L^{3-} ligand, one oxygen atom from the η^2-AcO^- bridging ligand, two oxygen atoms from one AcO^- terminal ligand, and two oxygen atoms provided by one F_6acac^- terminal ligand; meanwhile, the Dy4 atom is bonded by one oxygen atom of the η^3-CH_2O^- group, one oxygen atom of the η^2-CH_2O^- group from one H_3L^{3-} ligand, one oxygen atom of the η^3-CH_2O^- group from another H_3L^{3-} ligand, one oxygen atom of one η^2-AcO^- bridging ligand, and four oxygen atoms supplied by two F_6acac^- terminal ligands. After SHAPE software[68] analysis, the coordination geometries of the two Dy(III) cations were determined to be the square antiprism, with the deviations from the D_{4d} symmetry of 1.530 for the Dy1 atom (Table S3) and 1.418 for the Dy4 atom (Table S4). The Dy–N bond distances (mean 2.535 Å, Table 2) of **1** are a little shorter than those in $[Dy_4(H_3L)_2(OAc)_6]\cdot 2EtOH$ (average 2.584 Å),[57] and the Dy–O bond distances (mean 2.390 Å, Table 2) of **1** are comparable with those in $[Dy_4(H_3L)_2(OAc)_6]\cdot 2EtOH$ (average 2.397 Å).[57]

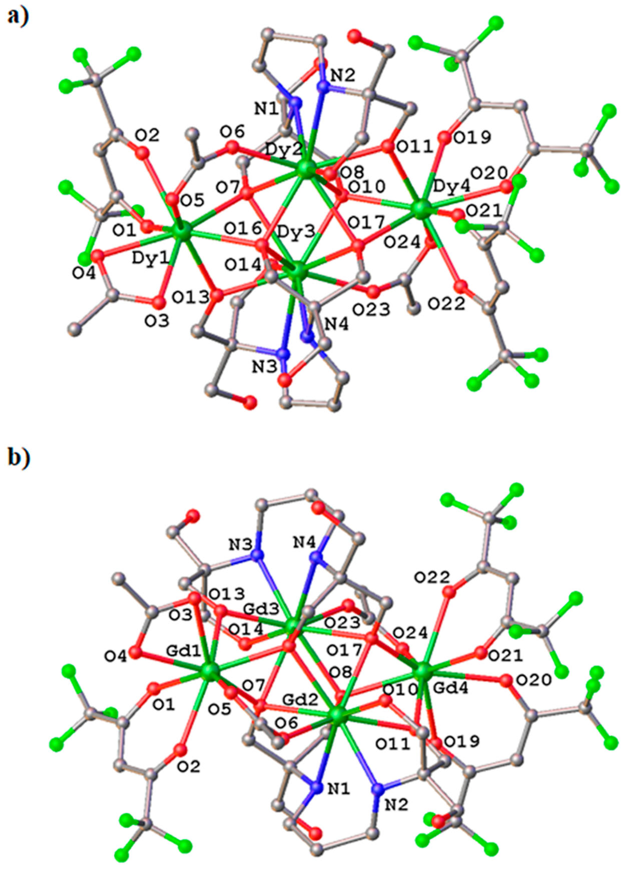

Figure 1. Crystal structures of **1** (a) and **2** (b). All H atoms and lattice H_2O and MeOH molecules are not shown for clarity.

Moreover, there exist extensive hydrogen bonds between lattice methanol molecules, between lattice water molecules, and between the lattice molecule (MeOH or H_2O) and the cluster molecule (Figure S1), these weak intermolecular interactions act to stabilize the crystal structure.

The structure of complex **2** (Figure 1b) is very similar to that of complex **1** (Figure 1a). However, the Gd–N bond lengths for **2** (average 2.557 Å, Table 2) are slightly longer than the Dy–N bond distances for **1** (average 2.536 Å, Table 2), and the Gd–O bond lengths (mean 2.413 Å, Table 2) for **2** are also larger than the Dy–O bond distances for **1** (average 2.390 Å, Table 2) because of the lanthanide contraction effect.

Notably, there are three acetate ligands and three hexafluoroacetylacetonate ligands in the molecules of complexes **1** and **2**; these different ligands cannot be symmetrically distributed on both sides of the Ln_4 cluster core, which thus causes the whole molecule to lose its centrosymmetry. Complexes **1** and **2** represent the first chiral Ln(III) cluster complexes constructed by the asymmetric distribution of different achiral ligands on both sides of the cluster core.

Magnetic Properties. Variable temperature dc magnetic susceptibilities of both complexes (Figure 2) showed that the χT values at 300 K are 56.61 $cm^3\ kmol^{-1}$ for **1** and 31.56 $cm^3\ kmol^{-1}$ for **2**, which are in good agreement with the calculated values of 56.68 $cm^3\ kmol^{-1}$ for the four uncoupled Dy^{3+} ions and 31.75 $cm^3\ kmol^{-1}$ for the four isolated Gd^{3+} ions, respectively. As the temperature decreases, their χT values start to decrease slowly at first, then decrease sharply at about 25 K, and the values at 2 K are 23.94 $cm^3\ kmol^{-1}$ for **1** and 14.19 $cm^3\ kmol^{-1}$ for **2**. The $1/\chi - T$ data of **2** conform to the Curie–Weiss law (Figure S2). After being fitted, the C value of 31.66 $cm^3\ kmol^{-1}$ and the θ value of −2.15 K were given for **2**. This negative and small θ value indicates that there exists weak antiferromagnetic coupling among the Gd^{3+} ions. The $1/\chi - T$ data of **1** can also be fitted using the Curie–Weiss law to obtain the θ value of −4.01 K and the C value of 57.01 $cm^3\ kmol^{-1}$ (Figure S3). The negative and small θ value of **1** implies that besides the thermal depopulation of m_j levels of the Dy^{3+} ion, there may also be weak antiferromagnetic coupling among the Ln^{3+} ions in **1**, similar to **2**.

The field-dependent magnetization of both complexes at different temperatures was measured too. For **1**, the $M-H/T$ plots do not overlap at 2–6 K (Figure S4), indicating that **1** has magnetic anisotropy, which is generally beneficial for SMM properties.

https://doi.org/10.1021/acsomega.2c02155
ACS Omega 2022, 7, 20229–20236

Table 2. Selected Bond Lengths (Å) and Angles (Deg) for 1 and 2

complex 1			
Dy1−O1	2.442(12)	Dy1−O2	2.392(14)
Dy1−O3	2.473(13)	Dy1−O4	2.395(8)
Dy1−O5	2.391(14)	Dy1−O7	2.324(12)
Dy1−O13	2.268(12)	Dy1−O16	2.345(12)
Dy2−O6	2.378(12)	Dy2−O7	2.457(11)
Dy2−O8	2.442(12)	Dy2−O10	2.367(12)
Dy2−O11	2.295(11)	Dy2−O16	2.418(12)
Dy2−O17	2.534(11)	Dy2−N1	2.473(14)
Dy2−N2	2.585(15)	Dy3−O7	2.512(13)
Dy3−O8	2.411(11)	Dy3−O13	2.285(11)
Dy3−O14	2.446(12)	Dy3−O16	2.421(11)
Dy3−O17	2.455(12)	Dy3−O23	2.318(13)
Dy3−N3	2.572(13)	Dy3−N4	2.509(14)
Dy4−O8	2.365(11)	Dy4−O11	2.295(11)
Dy4−O17	2.261(12)	Dy4−O19	2.410(14)
Dy4−O20	2.433(10)	Dy4−O21	2.405(14)
Dy4−O22	2.374(14)	Dy4−O24	2.399(12)
N1−Dy2−N2	73.3(4)	N4−Dy3−N3	74.6(4)
Dy1−O7−Dy2	106.0(5)	Dy1−O7−Dy3	93.7(4)
Dy2−O7−Dy3	84.7(4)	Dy3−O8−Dy2	87.3(4)
Dy4−O8−Dy2	94.6(4)	Dy4−O8−Dy3	106.3(5)
Dy4−O11−Dy2	101.3(4)	Dy1−O13−Dy3	101.7(4)
Dy1−O16−Dy2	106.6(5)	Dy1−O16−Dy3	95.6(4)
Dy2−O16−Dy3	87.6(4)	Dy3−O17−Dy2	84.3(4)
Dy4−O17−Dy2	94.8(4)	Dy4−O17−Dy3	108.2(4)
complex 2			
Gd1−O1	2.469(16)	Gd1−O2	2.380(16)
Gd1−O3	2.458(18)	Gd1−O4	2.412(14)
Gd1−O5	2.462(14)	Gd1−O7	2.343(14)
Gd1−O13	2.300(15)	Gd1−O16	2.359(14)
Gd2−O6	2.402(16)	Gd2−O7	2.508(14)
Gd2−O8	2.465(14)	Gd2−O10	2.405(16)
Gd2−O11	2.344(14)	Gd2−O16	2.475(14)
Gd2−O17	2.505(14)	Gd2−N1	2.509(17)
Gd2−N2	2.593(17)	Gd3−O7	2.538(15)
Gd3−O8	2.416(14)	Gd3−O13	2.289(14)
Gd3−O14	2.458(14)	Gd3−O16	2.430(14)
Gd3−O17	2.464(14)	Gd3−O23	2.351(16)
Gd3−N3	2.596(16)	Gd3−N4	2.529(17)
Gd4−O8	2.388(14)	Gd4−O11	2.289(15)
Gd4−O17	2.325(14)	Gd4−O19	2.468(18)
Gd4−O20	2.456(14)	Gd4−O21	2.429(18)
Gd4−O22	2.416(18)	Gd4−O24	2.392(16)
Gd1−O7−Gd2	105.3(6)	Gd1−O7−Gd3	93.7(5)
Gd2−O7−Gd3	84.1(4)	Gd3−O8−Gd2	87.7(4)
Gd4−O8−Gd2	94.6(5)	Gd4−O8−Gd3	107.2(5)
Gd4−O11−Gd2	100.7(5)	Gd3−O13−Gd1	101.9(5)
Gd1−O16−Gd2	105.8(5)	Gd1−O16−Gd3	96.2(5)
Gd3−O16−Gd2	87.1(4)	Gd3−O17−Gd2	85.7(4)
Gd4−O17−Gd2	95.1(5)	Gd4−O17−Gd3	107.6(5)

Figure 3a shows the $M-H$ plots at 2−10 K of **2**, which can be used to evaluate the magnitude of the magnetocaloric effect. According to the Maxwell formula, $\Delta S_m(T)_{\Delta H} = \int[\partial M(T,H)/\partial T]_H dH$,[69] we could figure out the corresponding magnetic entropy change values of **2** at different temperatures under varied magnetic field differences (ΔH). Figure 3b reveals that the $-\Delta S_m$ value gradually increases both with increasing ΔH and with decreasing temperature. The largest $-\Delta S_m$ value of 21.88 J kg^{-1} K^{-1} occurs at 2 K when ΔH is 5 T, this value is smaller than the value of 31.43 J kg^{-1} K^{-1} calculated using the formula, $-\Delta S_m = nR\ln(2S + 1)$ (n = 4, S = 7/2 and the R value is 8.314 J mol^{-1} K^{-1}), owing to the antiferromagnetic interaction among Gd^{3+} ions in **2**. This value is larger in magnetic refrigeration molecule materials, and comparable with those of other Gd_4 cluster complexes when ΔH is 5 T.[70−75]

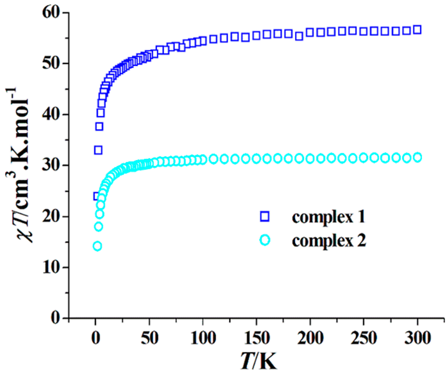

Figure 2. Plots of χT vs T of **1** and **2**.

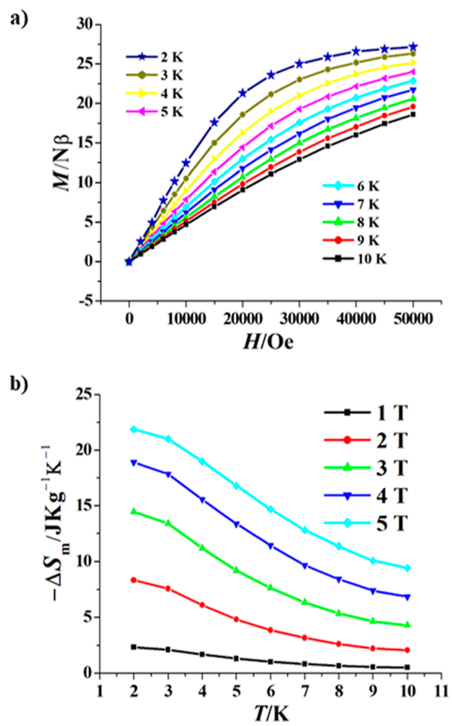

Figure 3. Magnetization vs field plots of **2** at 2−10 K (a); plots of $-\Delta S_m$ vs T of **2** (b).

As to the magnetic dynamics of **1**, we first measured the ac magnetic susceptibility of **1** under zero dc field. The temperature-dependent ac magnetic susceptibility indicates the $\chi''-T$ plots display frequency dependence and the trend of double magnetic relaxation, but the peak shape in the high-temperature region is not obvious (Figure S5). In order to investigate whether the existence of quantum tunneling effects prevents such peaks in the high-temperature region from appearing, we measured the magnetic field-dependent ac magnetic susceptibility at 13 K and 997 Hz (Figure S6). However, the optimal magnetic field has not been found.

https://doi.org/10.1021/acsomega.2c02155
ACS Omega 2022, 7, 20229−20236

Moreover, we tried to measure the ac magnetic susceptibility at 997 Hz under 1400 and 2000 Oe, and they also cannot form peaks around 13 K, similar to the ac magnetic susceptibility at 0 Oe (Figure S7), the quantum tunneling effect is thus excluded.

However, the frequency-dependent ac magnetic susceptibility at the 0 Oe field reveals that the $\chi''-\nu$ plots can show a temperature-dependent peak in a wide range of 2−14 K (Figure 4a), although there is also a trend of double magnetic relaxation. Using these data to plot the $\ln(\tau)$ versus $1/T$ curve (Figure 4b), it can be seen that the plot deviates significantly from the straight line at lower temperatures, indicating that besides the Orbach process, the magnetic relaxation also has the two-phonon Raman process. Therefore, we fitted this curve with the equation $\tau^{-1} = \tau_0^{-1}\exp(-U_{eff}/kT) + CT^n$ including both the Raman process and the Orbach process, yielding n = 1.67, C = 12.39 s^{-1} $K^{-1.67}$, $\tau_0 = 4.9 \times 10^{-6}$ s, and U_{eff}/k = 48.4 K. The large C value of **1** suggests that the Raman process is more prominent in the magnetic relaxation.[76] Furthermore, the Raman process can also be seen in the $\chi''-\nu$ plots (Figure 4a), which show not only the broad peak shape at low temperature but also the high-frequency plateau shape with increasing temperature.[77−79] The τ_0 value of 4.9×10^{-6} s is a normal value for SMMs.[1] The U_{eff}/k value (48.4 K) is comparable with that of the fast Orbach process (44.0 K) but smaller than that of the slow Orbach process in $[Dy_4(H_3L)_2(OAc)_6]\cdot 2EtOH$ (107.0 K).[57]

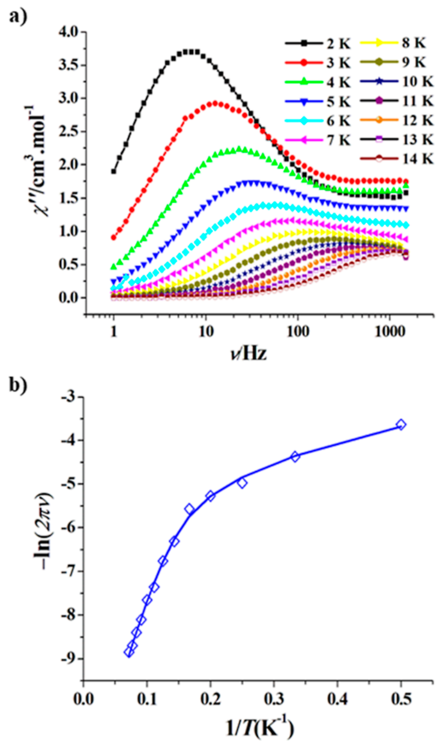

Figure 4. Frequency dependence of χ'' for **1** at zero dc field (a); $\ln(\tau)$ vs $1/T$ plot for **1**, the solid line represents the best fitting (b).

In addition, the Cole−Cole curves in the $\chi''-\chi'$ plots show partial characteristics of the double magnetic relaxation (Figure S8), which are not surprising because **1** contains Dy^{3+} ions in two coordination configurations, and the Cole−Cole plots at 2−14 K could be fitted by the formula containing two Debye functions.[57,80,81] The fitting results showed that its α_1 value range is 0.15−0.41 and its α_2 value range is 0.33−0.56 (Table S5). The larger values of α_1 and α_2 may be closely related to the obvious Raman mechanism in the magnetic relaxation process.[38,76] There is no open hysteresis loop for **1** at 1.9 K (Figure S9).

■ CONCLUSIONS

In summary, two chiral Ln_4 cluster complexes derived from *N*,*N*′-(1,3-propanediyl)bis[*N*-[1,1-bis(hydroxymethyl)-2-hydroxyethyl]amine] were synthesized successfully although no chiral ligands were used. It is the asymmetric distribution of acetate ligands and hexafluoroacetylacetonate ligands on both sides of the parallelogram-like Ln_4 core, which leads to the chirality of the whole molecule. The Dy complex exhibits SMM properties at the zero field, including not only the Orbach process but also the Raman process. While the Gd complex has large magnetic entropy changes, it is a potential molecular material for magnetic refrigeration. This work demonstrates that the chiral Ln(III) cluster complexes can be constructed from achiral ligands through the asymmetric distribution of different ligands on both sides of the cluster core. More such chiral cluster molecular materials can be assembled by changing the ligands at both ends of the metal cluster core or changing the metal cluster core itself.

■ ASSOCIATED CONTENT

Supporting Information

The Supporting Information is available free of charge at https://pubs.acs.org/doi/10.1021/acsomega.2c02155.

Additional experimental details; materials and methods; continuous shape measures calculation for Dy atoms in **1**; unit cell packing diagram of **1**; χ^{-1} versus T plots for **1** and **2**; M versus H/T plots of **1**; temperature dependence of χ'' at a 0 Oe field for **1**; ac susceptibilities measured in a 2.5 Oe ac magnetic field with variable dc fields at 997 Hz and 13 K for **1**; temperature dependence of χ'' at 997 Hz under different dc fields for **1**; Cole−Cole plots and hysteresis loop for **1**; and linear combination of two modified Debye model fitting parameters of **1** (PDF)

Accession Codes

www.ccdc.cam.ac.uk/data_request/cif

■ AUTHOR INFORMATION

Corresponding Author

Cai-Ming Liu − *Beijing National Laboratory for Molecular Sciences, Center for Molecular Science, Key Laboratory of Organic Solids, Institute of Chemistry, Chinese Academy of Sciences, Beijing 100190, China; School of Chemical Sciences, University of Chinese Academy of Sciences, Beijing 100049, China*; orcid.org/0000-0001-7184-6693; Email: cmliu@iccas.ac.cn

Author

Xiang Hao − *Beijing National Laboratory for Molecular Sciences, Center for Molecular Science, Key Laboratory of Organic Solids, Institute of Chemistry, Chinese Academy of Sciences, Beijing 100190, China*

Complete contact information is available at: https://pubs.acs.org/10.1021/acsomega.2c02155

Notes

The authors declare no competing financial interest.

■ ACKNOWLEDGMENTS

We thank the National Natural Science Foundation of China (21871274) for funding this work.

■ REFERENCES

(1) Woodruff, D. N.; Winpenny, R. E. P.; Layfield, R. A. Lanthanide Single-Molecule Magnets. *Chem. Rev.* **2013**, *113*, 5110.
(2) Zheng, X.-Y.; Kong, X.-J.; Zheng, Z.; Long, L.-S.; Zheng, L.-S. High-Nuclearity Lanthanide-Containing Clusters as Potential Molecular Magnetic Coolers. *Acc. Chem. Res.* **2018**, *51*, 517.
(3) Zheng, Y.-Z.; Zhou, G.-J.; Zheng, Z.; Winpenny, R. E. P. Molecule-based magnetic coolers. *Chem. Soc. Rev.* **2014**, *43*, 1462.
(4) Chang, L.-X.; Xiong, G.; Wang, L.; Cheng, P.; Zhao, B. A 24-Gd nanocapsule with a large magnetocaloric effect. *Chem. Commun.* **2013**, *49*, 1055.
(5) Das, C.; Vaidya, S.; Gupta, T.; Frost, J. M.; Righi, M.; Brechin, E. K.; Affronte, M.; Rajaraman, G.; Shanmugam, M. Single-Molecule Magnetism, Enhanced Magnetocaloric Effect, and Toroidal Magnetic Moments in a Family of Ln_4 Squares. *Chem.—Eur. J.* **2015**, *21*, 15639.
(6) Liu, C.-M.; Zhang, D.-Q.; Hao, X.; Zhu, D.-B. Arraying Octahedral $\{Cr_2Dy_4\}$ Units into 3D Single-Molecule-Magnet-Like Inorganic Compounds with Sulfate Bridges. *Inorg. Chem.* **2018**, *57*, 6803.
(7) Pineda, E. M.; Lorusso, G.; Zangana, K. H.; Palacios, E.; Schnack, J.; Evangelisti, M.; Winpenny, R. E. P.; McInnes, E. J. L. Observation of the influence of dipolar and spin frustration effects on the magnetocaloric properties of a trigonal prismatic $\{Gd_7\}$ molecular nanomagnet. *Chem. Sci.* **2016**, *7*, 4891.
(8) Luo, X.-M.; Hu, Z.-B.; Lin, Q.-f.; Cheng, W.; Cao, J.-P.; Cui, C.-H.; Mei, H.; Song, Y.; Xu, Y. Exploring the Performance Improvement of Magnetocaloric Effect Based Gd-Exclusive Cluster Gd_{60}. *J. Am. Chem. Soc.* **2018**, *140*, 11219.
(9) Peng, J.-B.; Zhang, Q.-C.; Kong, X.-J.; Ren, Y.-P.; Long, L.-S.; Huang, R.-B.; Zheng, L.-S.; Zheng, Z. A 48-Metal Cluster Exhibiting a Large Magnetocaloric Effect. *Angew. Chem., Int. Ed.* **2011**, *50*, 10649.
(10) Guo, F.-S.; Chen, Y.-C.; Mao, L.-L.; Lin, W.-Q.; Leng, J.-D.; Tarasenko, R.; Orendáč, M.; Prokleška, J.; Sechovský, V.; Tong, M.-L. Anion-Templated Assembly and Magnetocaloric Properties of a Nanoscale $\{Gd_{38}\}$ Cage versus a $\{Gd_{48}\}$ Barrel. *Chem.—Eur. J.* **2013**, *19*, 14876.
(11) Liu, S.-J.; Zhao, J.-P.; Tao, J.; Jia, J.-M.; Han, S.-D.; Li, Y.; Chen, Y.-C.; Bu, X.-H. An Unprecedented Decanuclear Gd^{III} Cluster for Magnetic Refrigeration. *Inorg. Chem.* **2013**, *52*, 9163.
(12) Wang, K.; Chen, Z.-L.; Zou, H.-H.; Hu, K.; Li, H.-Y.; Zhang, Z.; Sun, W.-Y.; Liang, F.-P. A single-stranded $\{Gd_{18}\}$ nanowheel with a symmetric polydentate diacylhydrazone ligand. *Chem. Commun.* **2016**, *52*, 8297.
(13) Bogani, L.; Cavigli, L.; Bernot, K.; Sessoli, R.; Gurioli, M.; Gatteschi, D. Evidence of intermolecular π-stacking enhancement of second-harmonic generation in a family of single chain magnets. *J. Mater. Chem.* **2006**, *16*, 2587.
(14) Train, C.; Nuida, T.; Gheorghe, R.; Gruselle, M.; Ohkoshi, S.-i. Large Magnetization-Induced Second Harmonic Generation in an Enantiopure Chiral Magnet. *J. Am. Chem. Soc.* **2009**, *131*, 16838.
(15) Wen, H.-R.; Hu, J.-J.; Yang, K.; Zhang, J.-L.; Liu, S.-J.; Liao, J.-S.; Liu, C.-M. Family of Chiral Zn^{II}-Ln^{III} (Ln = Dy and Tb) Heterometallic Complexes Derived from the Amine-Phenol Ligand Showing Multifunctional Properties. *Inorg. Chem.* **2020**, *59*, 2811.
(16) Zhu, S.-D.; Hu, J.-J.; Dong, L.; Wen, H.-R.; Liu, S.-J.; Lu, Y.-B.; Liu, C.-M. Multifunctional Zn(ii)-Yb(iii) complex enantiomers showing second-harmonic generation, near-infrared luminescence, single-molecule magnet behaviour and proton conduction. *J. Mater. Chem. C* **2020**, *8*, 16032.
(17) Long, J.; Rouquette, J.; Thibaud, J.-M.; Ferreira, R. A. S.; Carlos, L. D.; Donnadieu, B.; Vieru, V.; Chibotaru, L. F.; Konczewicz, L.; Haines, J.; Guari, Y.; Larionova, J. A High-Temperature Molecular Ferroelectric Zn/Dy Complex Exhibiting Single-Ion-Magnet Behavior and Lanthanide Luminescence. *Angew. Chem., Int. Ed.* **2015**, *54*, 2236.
(18) Li, D.-P.; Wang, T.-W.; Li, C.-H.; Liu, D.-S.; Li, Y.-Z.; You, X.-Z. Single-ion magnets based on mononuclear lanthanide complexes with chiral Schiff base ligands $[Ln(FTA)_3L]$ (Ln = Sm, Eu, Gd, Tb and Dy). *Chem. Commun.* **2010**, *46*, 2929.
(19) Li, X.-L.; Chen, C.-L.; Gao, Y.-L.; Liu, C.-M.; Feng, X.-L.; Gui, Y.-H.; Fang, S.-M. Modulation of Homochiral Dy III Complexes: Single-Molecule Magnets with Ferroelectric Properties. *Chem.—Eur. J.* **2012**, *18*, 14632.
(20) Li, X.-L.; Hu, M.; Yin, Z.; Zhu, C.; Liu, C.-M.; Xiao, H.-P.; Fang, S. Enhanced single-ion magnetic and ferroelectric properties of mononuclear Dy(iii) enantiomeric pairs through the coordination role of chiral ligands. *Chem. Commun.* **2017**, *53*, 3998.
(21) Rikken, G. L. J. A.; Raupach, E. Observation of magneto-chiral dichroism. *Nature* **1997**, *390*, 493.
(22) Train, C.; Gheorghe, R.; Krstic, V.; Chamoreau, L.-M.; Ovanesyan, N. S.; Rikken, G. L. J. A.; Gruselle, M.; Verdaguer, M. Strong magneto-chiral dichroism in enantiopure chiral ferromagnets. *Nat. Mater.* **2008**, *7*, 729.
(23) Kitagawa, Y.; Segawa, H.; Ishii, K. Magneto-Chiral Dichroism of Organic Compounds. *Angew. Chem., Int. Ed.* **2011**, *50*, 9133.
(24) Atzori, M.; Santanni, F.; Breslavetz, I.; Paillot, K.; Caneschi, A.; Rikken, G. L. J. A.; Sessoli, R.; Train, C. Magnetic Anisotropy Drives Magnetochiral Dichroism in a Chiral Molecular Helix Probed with Visible Light. *J. Am. Chem. Soc.* **2020**, *142*, 13908.
(25) Wang, K.; Zeng, S.; Wang, H.; Dou, J.; Jiang, J. Magneto-chiral dichroism in chiral mixed (phthalocyaninato)(porphyrinato) rare earth triple-decker SMMs. *Inorg. Chem. Front.* **2014**, *1*, 167.
(26) Wang, X.; Du, M.-H.; Xu, H.; Long, L.-S.; Kong, X.-J.; Zheng, L.-S. Cocrystallization of Chiral 3d-4f Clusters $\{Mn_{10}Ln_6\}$ and $\{Mn_6Ln_2\}$. *Inorg. Chem.* **2021**, *60*, 5925.
(27) Liu, C.-M.; Sun, R.; Wang, B.-W.; Wu, F.; Hao, X.; Shen, Z. Homochiral Ferromagnetic Coupling Dy_2 Single-Molecule Magnets with Strong Magneto-Optical Faraday Effects at Room Temperature. *Inorg. Chem.* **2021**, *60*, 12039.
(28) Numata, Y.; Inoue, K.; Baranov, N.; Kurmoo, M.; Kikuchi, K. Field-Induced Ferrimagnetic State in a Molecule-Based Magnet Consisting of a Co^{II} Ion and a Chiral Triplet Bis(nitroxide) Radical. *J. Am. Chem. Soc.* **2007**, *129*, 9902.
(29) Feng, J.-S.; Ren, M.; Cai, Z.-S.; Fan, K.; Bao, S.-S.; Zheng, L.-M. Enantiopure phosphonic acids as chiral inducers: homochiral crystallization of cobalt coordination polymers showing field-induced slow magnetization relaxation. *Chem. Commun.* **2016**, *52*, 6877.
(30) Yao, M.-X.; Zheng, Q.; Gao, F.; Li, Y.-Z.; Song, Y.; Zuo, J.-L. Field-induced slow magnetic relaxation in chiral seven-coordinated mononuclear lanthanide complexes. *Dalton Trans.* **2012**, *41*, 13682.
(31) El Rez, B.; Liu, J.; Béreau, V.; Duhayon, C.; Horino, Y.; Suzuki, T.; Coolen, L.; Sutter, J.-P. Concomitant emergence of circularly polarized luminescence and single-molecule magnet behavior in chiral-at-metal Dy complex. *Inorg. Chem. Front.* **2020**, *7*, 4527.
(32) Feng, M.; Lyu, B.-H.; Wang, M.-H.; Wu, W.-W.; Chen, Y.-C.; Huang, G.-Z.; Lin, W.-Q.; Wu, S.-G.; Liu, J.-L.; Tong, M.-L. Chiral Erbium(III) Complexes: Single-Molecule Magnet Behavior, Chirality, and Nuclearity Control. *Inorg. Chem.* **2019**, *58*, 10694.
(33) Liu, C.-M.; Zhang, D.-Q.; Zhu, D.-B. Field-Induced Single-Ion Magnets Based on Enantiopure Chiral β-Diketonate Ligands. *Inorg. Chem.* **2013**, *52*, 8933.
(34) Lang, W.-J.; Kurmoo, M.; Zeng, M.-H. A Chiral and Polar Single-Molecule Magnet: Synthesis, Structure, and Tracking of Its Formation Using Mass Spectrometry. *Inorg. Chem.* **2019**, *58*, 7236.
(35) Casanovas, B.; Speed, S.; El Fallah, M. S.; Vicente, R.; Font-Bardía, M.; Zinna, F.; Di Bari, L. Chiral dinuclear Ln(iii) complexes derived from *S*- and *R*-2-(6-methoxy-2-naphthyl)propionate. Optical and magnetic properties. *Dalton Trans.* **2019**, *48*, 2059.
(36) Liu, C.-M.; Zhang, D.; Hao, X.; Zhu, D. Enantiopure Chiral Two-dimensional Sinusoidal Lanthanide(III) Coordination Polymers

Based on *R-/S*-2-Methylglutarate: Luminescence, Magnetic Entropy Change, and Magnetic Relaxation. *Cryst. Growth Des.* **2019**, *19*, 4731.
(37) Zhu, Y.-Y.; Guo, X.; Cui, C.; Wang, B.-W.; Wang, Z.-M.; Gao, S. An enantiopure Fe^{III}_4 single-molecule magnet. *Chem. Commun.* **2011**, *47*, 8049.
(38) Liu, C.-M.; Sun, R.; Hao, X.; Wang, B. Chiral Co-Crystals of (*S*)- or (*R*)-1,1′-Binaphthalene-2,2′-diol and Zn_2Dy_2 Tetranuclear Complexes Behaving as Single-Molecule Magnets. *Cryst. Growth Des.* **2021**, *21*, 4346.
(39) Liu, C.-M.; Zhang, D.-Q.; Xiong, R.-G.; Hao, X.; Zhu, D.-B. A homochiral Zn-Dy heterometallic left-handed helical chain complex without chiral ligands: anion-induced assembly and multifunctional integration. *Chem. Commun.* **2018**, *54*, 13379.
(40) Liu, M.-J.; Yuan, J.; Wang, B.-L.; Wu, S.-T.; Zhang, Y.-Q.; Liu, C.-M.; Kou, H.-Z. Spontaneous Resolution of Chiral Co(III)Dy(III) Single-Molecule Magnet Based on an Achiral Flexible Ligand. *Cryst. Growth Des.* **2018**, *18*, 7611.
(41) Liu, C.-M.; Zhang, D.-Q.; Hao, X.; Zhu, D.-B. Assembly of chiral 3d-4f wheel-like cluster complexes with achiral ligands: single-molecule magnetic behavior and magnetocaloric effect. *Inorg. Chem. Front.* **2020**, *7*, 3340.
(42) Lin, P.-H.; Burchell, T. J.; Ungur, L.; Chibotaru, L. F.; Wernsdorfer, W.; Murugesu, M. Single-Molecule Magnets. *Angew. Chem., Int. Ed.* **2009**, *48*, 9489.
(43) Zheng, Y.-Z.; Lan, Y.; Anson, C. E.; Powell, A. K. Anion-Perturbed Magnetic Slow Relaxation in Planar $\{Dy_4\}$ Clusters. *Inorg. Chem.* **2008**, *47*, 10813.
(44) Bi, Y.; Wang, X.-T.; Liao, W.; Wang, X.; Deng, R.; Zhang, H.; Gao, S. Thiacalix[4]arene-Supported Planar Ln_4 (Ln = Tb^{III}, Dy^{III}) Clusters: Toward Luminescent and Magnetic Bifunctional Materials. *Inorg. Chem.* **2009**, *48*, 11743.
(45) Gao, Y.; Xu, G.-F.; Zhao, L.; Tang, J.; Liu, Z. Observation of Slow Magnetic Relaxation in Discrete Dysprosium Cubane. *Inorg. Chem.* **2009**, *48*, 11495.
(46) Abbas, G.; Lan, Y.; Kostakis, G. E.; Wernsdorfer, W.; Anson, C. E.; Powell, A. K. Series of Isostructural Planar Lanthanide Complexes $[Ln^{III}_4(\mu_3\text{-OH})_2(mdeaH)_2(piv)_8]$ with Single Molecule Magnet Behavior for the Dy_4 Analogue. *Inorg. Chem.* **2010**, *49*, 8067.
(47) Yan, P.-F.; Lin, P.-H.; Habib, F.; Aharen, T.; Murugesu, M.; Deng, Z.-P.; Li, G.-M.; Sun, W.-B. Series of Isostructural Planar Lanthanide Complexes $[Ln^{III}_4(\mu_3\text{-OH})_2(mdeaH)_2(piv)_8]$ with Single Molecule Magnet Behavior for the Dy_4 Analogue. *Inorg. Chem.* **2011**, *50*, 7059.
(48) Guo, P.-H.; Liu, J.-L.; Zhang, Z.-M.; Ungur, L.; Chibotaru, L. F.; Leng, J.-D.; Guo, F.-S.; Tong, M.-L. The First $\{Dy_4\}$ Single-Molecule Magnet with a Toroidal Magnetic Moment in the Ground State. *Inorg. Chem.* **2012**, *51*, 1233.
(49) Woodruff, D. N.; Tuna, F.; Bodensteiner, M.; Winpenny, R. E. P.; Layfield, R. A. Single-Molecule Magnetism in Tetrametallic Terbium and Dysprosium Thiolate Cages. *Organometallics* **2013**, *32*, 1224.
(50) Acharya, J.; Biswas, S.; van Leusen, J.; Kumar, P.; Kumar, V.; Narayanan, R. S.; Kögerler, P.; Chandrasekhar, V. Exploring Tuning of Structural and Magnetic Properties by Modification of Ancillary *β*-Diketonate Co-ligands in a Family of Near-Linear Tetranuclear Dy^{III} Complexes. *Cryst. Growth Des.* **2018**, *18*, 4004.
(51) Langley, S. K.; Chilton, N. F.; Gass, I. A.; Moubaraki, B.; Murray, K. S. Planar tetranuclear lanthanide clusters with the Dy_4 analogue displaying slow magnetic relaxation. *Dalton Trans.* **2011**, *40*, 12656.
(52) Gass, I. A.; Moubaraki, B.; Langley, S. K.; Batten, S. R.; Murray, K. S. A *π*−*π* 3D network of tetranuclear μ_2/μ_3-carbonato Dy(III) bis-pyrazolylpyridine clusters showing single molecule magnetism features. *Chem. Commun.* **2012**, *48*, 2089.
(53) Xue, S.; Zhao, L.; Guo, Y.-N.; Deng, R.; Guo, Y.; Tang, J. A series of tetranuclear lanthanide complexes comprising two edge-sharing triangular units with field-induced slow magnetic relaxation for Dy_4 species. *Dalton Trans.* **2011**, *40*, 8347.
(54) Wu, S.-Q.; Xie, Q.-W.; An, G.-Y.; Chen, X.; Liu, C.-M.; Cui, A.-L.; Kou, H.-Z. Supramolecular lanthanide metallogrids exhibiting field-induced single-ion magnetic behavior. *Dalton Trans.* **2013**, *42*, 4369.
(55) Wang, W.-M.; Wu, Z.-L.; Zhang, Y.-X.; Wei, H.-Y.; Gao, H.-L.; Cui, J.-Z. Self-assembly of tetra-nuclear lanthanide clusters via atmospheric CO_2 fixation: interesting solvent-induced structures and magnetic relaxation conversions. *Inorg. Chem. Front.* **2018**, *5*, 2346.
(56) Liu, C.-M.; Zhang, D.-Q.; Hao, X.; Zhu, D.-B. Syntheses, Crystal Structures, and Magnetic Properties of Two p-tert-Butylsulfonylcalix[4]arene Supported Cluster Complexes with a Totally Disordered $Ln_4(OH)_4$ Cubane Core. *Cryst. Growth Des.* **2012**, *12*, 2948.
(57) Liu, C.-M.; Zhang, D.-Q.; Zhu, D.-B. A single-molecule magnet featuring a parallelogram $[Dy_4(OCH_2-)_4]$ core and two magnetic relaxation processes. *Dalton Trans.* **2013**, *42*, 14813.
(58) Xu, H.-B.; Zhong, Y.-T.; Zhang, W.-X.; Chen, Z.-N.; Chen, X.-M. Syntheses, structures and photophysical properties of hetero-trinuclear Zn_2Ln clusters (Ln = Nd, Eu, Tb, Er, Yb). *Dalton Trans.* **2010**, *39*, 5676.
(59) Liu, C.-M.; Zhang, D.-Q.; Hao, X.; Zhu, D.-B. Zn_2Ln_2 complexes with carbonate bridges formed by the fixation of carbon dioxide in the atmosphere: single-molecule magnet behaviour and magnetocaloric effect. *Dalton Trans.* **2020**, *49*, 2121.
(60) Liu, C.-M.; Zhang, D.-Q.; Zhu, D.-B. Hexanuclear $[Ni_2Ln_4]$ clusters exhibiting enhanced magnetocaloric effect and slow magnetic relaxation. *RSC Adv.* **2014**, *4*, 53870.
(61) Ferguson, A.; Darwish, A.; Graham, K.; Schmidtmann, M.; Parkin, A.; Murrie, M. Bis-Tris Propane as a New Polydentate Linker in the Synthesis of Iron(III) and Manganese(II/III) Complexes. *Inorg. Chem.* **2008**, *47*, 9742.
(62) Ferguson, A.; Schmidtmann, M.; Brechin, E. K.; Murrie, M. Bis-tris propane as a new multidentate ligand for nickel- and cobalt-based spin clusters. *Dalton Trans.* **2011**, *40*, 334.
(63) Milway, V. A.; Tuna, F.; Farrell, A. R.; Sharp, L. E.; Parsons, S.; Murrie, M. Directed Synthesis of $\{Mn_{18}Cu_6\}$ Heterometallic Complexes. *Angew. Chem., Int. Ed.* **2013**, *52*, 1949.
(64) Iman, K.; Raza, M. K.; Ansari, M.; Monika, A.; Ansari, A.; Ahmad, M.; Ahamad, M. N.; Qasem, K. M. A.; Hussain, S.; Akhtar, M. N.; Shahid, M. Novel $\{Cu_4\}$ and $\{Cu_4Cd_6\}$ clusters derived from flexible aminoalcohols: synthesis, characterization, crystal structures, and evaluation of anticancer properties. *Dalton Trans.* **2021**, *50*, 11941.
(65) Heras Ojea, M. J.; Milway, V. A.; Velmurugan, G.; Thomas, L. H.; Coles, S. J.; Wilson, C.; Wernsdorfer, W.; Rajaraman, G.; Murrie, M. Enhancement of Tb^{III}-Cu^{II} Single-Molecule Magnet Performance through Structural Modification. *Chem.—Eur. J.* **2016**, *22*, 12839.
(66) Liu, C.-M.; Zhang, D.-Q.; Zhu, D.-B. Fine Tuning the Energy Barrier of Molecular Nanomagnets via Lattice Solvent Molecules. *Sci. Rep.* **2017**, *7*, 15483.
(67) Han, S.-D.; Liu, S.-J.; Wang, Q.-L.; Miao, X.-H.; Hu, T.-L.; Bu, X.-H. Synthesis and Magnetic Properties of a Series of Octanuclear $[Fe_6Ln_2]$ Nanoclusters. *Cryst. Growth Des.* **2015**, *15*, 2253.
(68) Casanova, D.; Llunell, M.; Alemany, P.; Alvarez, S. The Rich Stereochemistry of Eight-Vertex Polyhedra: a Continuous Shape Measures Study. *Chem.—Eur. J.* **2005**, *11*, 1479.
(69) Pecharsky, V. K.; Gschneidner, K. A. Magnetocaloric effect and magnetic refrigeration. *J. Magn. Magn. Mater.* **1999**, *200*, 44.
(70) Chen, H.-M.; Wang, W.-M.; Li, X.-Q.; Chu, X.-Y.; Nie, Y.-Y.; Liu, Z.; Huang, S.-X.; Shen, H.-Y.; Cui, J.-Z.; Gao, H.-L. Luminescence and magnetocaloric effect of Ln_4 clusters (Ln = Eu, Gd, Tb, Er) bridged by CO_3^{2-} deriving from the spontaneous fixation of carbon dioxide in the atmosphere. *Inorg. Chem. Front.* **2018**, *5*, 394.
(71) Gao, H.-L.; Zhou, X.-P.; Bi, Y.-X.; Shen, H.-Y.; Wang, W.-M.; Wang, N.-N.; Chang, Y.-X.; Zhang, R.-X.; Cui, J.-Z. A Dy_4 single-molecule magnet and its Gd(iii), Tb(iii), Ho(iii), and Er(iii) analogues encapsulated by an 8-hydroxyquinoline Schiff base derivative and *β*-diketonate coligand. *Dalton Trans.* **2017**, *46*, 4669.

(72) Wang, W.-M.; Wu, Z.-L.; Cui, J.-Z. Molecular assemblies from linear-shaped Ln_4 clusters to Ln_8 clusters using different β-diketonates: disparate magnetocaloric effects and single-molecule magnet behaviours. *Dalton Trans.* **2021**, *50*, 12931.

(73) Rasamsetty, A.; Das, C.; Sañudo, E. C.; Shanmugam, M.; Baskar, V. Effect of coordination geometry on the magnetic properties of a series of Ln_2 and Ln_4 hydroxo clusters. *Dalton Trans.* **2018**, *47*, 1726.

(74) Sheikh, J. A.; Adhikary, A.; Konar, S. Magnetic refrigeration and slow magnetic relaxation in tetranuclear lanthanide cages (Ln = Gd, Dy) with in situ ligand transformation. *New J. Chem.* **2014**, *38*, 3006.

(75) Wang, W.-M.; Wang, M.-J.; Hao, S.-S.; Shen, Q.-Y.; Wang, M.-L.; Liu, Q.-L.; Guan, X.-F.; Zhang, X.-T.; Wu, Z.-L. 'Windmill'-shaped Ln^{III}_4 (Ln^{III} = Gd and Dy) clusters: magnetocaloric effect and single-molecule-magnet behavior. *New J. Chem.* **2020**, *44*, 4631.

(76) Lacelle, T.; Brunet, G.; Holmberg, R. J.; Gabidullin, B.; Murugesu, M. Holmberg, Bulat Gabidullin, and Muralee Murugesu, Unprecedented Octanuclear Dy^{III} Cluster Exhibiting Single-Molecule Magnet Behavior. *Cryst. Growth Des.* **2017**, *17*, 5044.

(77) Long, J.; Tolpygin, A. O.; Cherkasov, A. V.; Lyssenko, K. A.; Guari, Y.; Larionova, J.; Trifonov, A. A. Investigation of the slow relaxation of the magnetization dynamics in homoleptic ene-diamido organodysprosium(III) complexes with K^+/arene interactions. *CrystEngComm* **2020**, *22*, 4260.

(78) Long, J.; Tolpygin, A. O.; Cherkasov, A. V.; Lyssenko, K. A.; Guari, Y.; Larionova, J.; Trifonov, A. A. Single-Molecule Magnet Behavior in Dy^{3+} Half-Sandwich Complexes Based on Ene-Diamido and Cp* Ligands. *Organometallics* **2019**, *38*, 748.

(79) Long, J.; Shestakov, B. G.; Liu, D.; Chibotaru, L. F.; Guari, Y.; Cherkasov, A. V.; Fukin, G. K.; Trifonov, A. A.; Larionova, J. An organolanthanide(iii) single-molecule magnet with an axial crystal-field: influence of the Raman process over the slow relaxation. *Chem. Commun.* **2017**, *53*, 4706.

(80) Guo, Y.-N.; Xu, G.-F.; Gamez, P.; Zhao, L.; Lin, S.-Y.; Deng, R.; Tang, J.; Zhang, H.-J. Two-Step Relaxation in a Linear Tetranuclear Dysprosium(III) Aggregate Showing Single-Molecule Magnet Behavior. *J. Am. Chem. Soc.* **2010**, *132*, 8538.

(81) Langley, S. K.; Chilton, N. F.; Moubaraki, B.; Murray, K. S. Single-Molecule Magnetism in Three Related $\{Co^{III}_2Dy^{III}_2\}$-Acetylacetonate Complexes with Multiple Relaxation Mechanisms. *Inorg. Chem.* **2013**, *52*, 7183.

https://doi.org/10.1021/acsomega.2c02155
ACS Omega 2022, 7, 20229−20236